

Performance and durability of thin film solar cells via testing the abrasion resistance of broadband anti-reflection coatings

Sibel Yılmaz Ekinci 

Düzce University, Düzce, Türkiye, sibelyilmaz@duzce.edu.tr

Seda Sancaklı Atun 

Düzce University, Düzce, Türkiye, sedasancakli@gmail.com

Adam Michael Law 

Loughborough University, Leicestershire, UK, a.law@lboro.ac.uk

John Michael Walls 

Loughborough University, Leicestershire, UK, j.m.walls@lboro.ac.uk

Submitted: 14.06.2021

Accepted: 10.12.2021

Published: 31.03.2021



Abstract: Reflection from the front glass of solar modules causes over 4% optical loss leading to a significant decrease in module efficiency. Single layer solution gelation (sol-gel) anti-reflective (AR) coatings are effective over a narrow range of wavelengths, whereas reflection losses can be reduced over a broader wavelength when multilayer broadband AR coatings are applied. In this work, three different multilayer AR coatings including 4-layer SiO₂/ZrO₂, 4-layer SiO₂/ITO, and 6-layer SiO₂/ZrO₂ were deposited using magnetron sputtering. The abrasion resistance is important because the coatings will be subject to regular cleaning cycles. A variety of abrasers including Felt pad, CS-10 and CS-8 under different loads are used. The optical performance and durability of these coatings were analyzed using a spectrophotometer, optical microscope, scanning electron microscope, and scanning white light interferometer. No damage was observed after abrasion of the coatings with a felt pad under 1 and 2 N loads. However, there was a slight increase in Weighted Average Reflection. When coatings were tested with CS-10 and CS-8 abrasers, coatings with ZrO₂ resulted in higher scratch resistance in comparison to coating with ITO. However, all-dielectric broadband AR coatings are more durable and have better optical performance compared to single layer sol-gel coatings.

Keywords: Abrasion resistance, Anti-reflection (AR) coating, Photovoltaic (PV)

Cite this paper as: Yılmaz Ekinci, S., Atun Sancaklı, S., Law, A.M., & Walls, J.M., Performance and durability of thin film solar cells via testing the abrasion resistance of broadband anti-reflection coatings. *Journal of Energy Systems* 2022; 6(1): 33-45, DOI: 10.30521/jes.952231

© 2022 Published by peer-reviewed open access scientific journal, JES at DergiPark (<https://dergipark.org.tr/en/pub/jes>)

Nomenclature	
<i>3D</i>	Three-dimensional
<i>AR</i>	Anti-reflective
<i>CdTe</i>	Cadmium Telluride
<i>CIGS</i>	Copper Indium Gallium Di-selenide
<i>c-Si</i>	Crystalline Silicon
<i>DI</i>	De-ionized
<i>FEG</i>	Field Emission Gun
<i>IR</i>	Infra-red
<i>I_{sc}</i>	Short Circuit Current
<i>ITO</i>	Indium Tin Oxide
<i>Nb₂O₅</i>	Niobium Pentoxide
<i>O&M</i>	Operation and Management
<i>Pt</i>	Total height of the roughness profile
<i>PV</i>	Photovoltaic
<i>Rq</i>	Root-mean-square deviation of the roughness profile
<i>rms</i>	Root-mean-square
<i>Si</i>	Silicon
<i>SiO₂</i>	Silicon Dioxide
<i>SEM</i>	Scanning Electron Microscope
<i>Sol-gel</i>	Solution gelation
<i>SWLI</i>	Scanning White Light Interferometry
<i>TiO₂</i>	Titanium Dioxide
<i>WAR</i>	Weighted Average Reflection
<i>ZrO₂</i>	Zirconium Dioxide

1. INTRODUCTION

Generating electricity from photovoltaic (PV) systems is becoming a mainstream energy source. As deployment of solar increases, PV asset managers are starting to focus on operation and management (O&M) issues including the long-term performance durability and costs of maintenance. Losses in efficiency caused by the module cover glass are a major problem in solar utilities. The reflection losses from the front surface due to the refractive index difference between air and the glass substrate are >4% which limits the current generation from PV modules [1]. The first theory of reflection was derived in 1907 by Rayleigh [2]. To achieve low reflectance of a single layer anti-reflective (AR) coating, the thickness should be a quarter of the wavelength of incident light [3]. Single layer AR coatings are used in the PV industry and have gained significant market share to mitigate reflection losses [4,5]. Application of an AR coating can decrease these optical losses and increase the power output. However, the durability of the AR coatings exposed outdoors is a significant issue since PV modules are warranted for between 25 and 30 years [6,7]. Single layer porous silica coatings rely on the introduction of voids to achieve a low refractive index. The voids introduce vulnerability to water ingress and also reduce abrasion resistance, and these single-layer coatings have been found to be vulnerable to abrasion testing that simulates regular cleaning of modules [8,9]. Multilayer, all-dielectric, AR coatings have been developed to overcome these limitations [10].

The PV industry is dominated by crystalline silicon (c-Si) and thin film solar cells including copper indium gallium di-selenide (CIGS) and cadmium telluride (CdTe) thin film devices [7]. The light is absorbed by soda lime glass at 350 nm and below this wavelength [11]. Thin film CdTe solar cells have a direct band gap of 1.45 eV and they can absorb wavelengths up to 850 nm. Therefore, wavelengths between 350 nm and 850 nm are used for power generation in thin film CdTe solar cells. [12] The losses caused by reflection are ~4% over a broad spectral range leading to an equivalent reduction in the short circuit current (I_{sc}) [13]. These losses can be reduced by ~70% relative using an AR coating [12]. Si absorbs light over a broader spectral range 350 nm to 1150 nm and a different design of AR coating is required. Recently a 6-layer coating design was reported that reduces the Weighted Average Reflection (WAR) by 2.3% absolute [14].

There are several techniques for depositing AR coatings such as solution gelation (sol-gel) [3], [15,16,17], thermal evaporation [15,16,18], sputtering [5,15,16], and electron beam [15,16,18]. Single layer sol-gel AR coatings are commonly used in the PV industry due to their low cost and fast manufacturing [16]; however, they minimise reflection at a single wavelength [16]. Sol-gel deposition methods require a low refractive index material, which can lead to lower scratch resistance [8]. Improving the scratch resistance of the sol-gel AR coatings may increase the refractive index and reduce the AR effect [8]. The mechanical properties such as hardness of coatings depend on the thickness of the material, where the hardness decreases with increasing the thickness [19].

Reflection losses can be reduced over a broader wavelength by the application of a multilayer broadband AR coating [7]. Optical properties are very sensitive to the thickness of the coatings to achieve broadband optical performance [19]. The mechanical issues associated with sol-gel can be avoided by using multilayer AR coatings. The design can be optimised for the required wavelength ranges using low and high refractive index materials [20]. Silicon dioxide (SiO_2) has a refractive index of 1.46 at 550 nm wavelength and it is commonly used as a low refractive index material. SiO_2 is chemically stable and scratch resistant [21]. There is a variety of high refractive index materials including zirconium dioxide (ZrO_2), titanium dioxide (TiO_2), or niobium pentoxide (Nb_2O_5). [8] Zr-based materials have high hardness, good wear resistance and improved temperature stability [22]. It is a crucial step to select the proper material for high index optical properties and durability of the coating. Multilayer AR coatings are widely used in the ophthalmic industry to reduce reflection [23], however further

investigation is required to adapt these coatings for use on PV modules. Three different coatings were used in this study, designated ‘A’, ‘B’ and ‘C’ (Table 1).

Coating A was designed to be deposited onto the superstrate of thin film CdTe solar cells to reduce the reflection losses, and has been shown to provide a 3.6% relative increase in power output. It is a 4-layer multilayer AR coating composed of SiO₂ and ZrO₂. The precise modelled thickness of coating A is 277 nm [8].

Coating B was optimized AR within the required wavelength range for silicon (Si) solar cells and this coating also limits the increase in the module temperature via reflecting infra-red (IR) radiation. Lower operating temperatures will lead to an increase in efficiency. The coating has 4-layer structure using SiO₂ as a low refractive index material and indium tin oxide (ITO) as a high index material. The precise modelled thickness was 274 nm. [24] In Si solar cells, increased operating temperature is responsible for a significant loss in efficiency [25]. To address this issue, coating B which reflects IR radiation was examined. ITO enables reflection of IR wavelengths at higher than 1300 nm [24]. Coating B which is a 4-layer multilayer coating comprising ITO and SiO₂ was designed to provide required anti-reflectivity for Si solar cells.

Coating C is a 6-layer AR coating for use on Si solar cells. It comprises SiO₂ and ZrO₂ materials with a total precise modelled thickness of 344 nm [14]. It is possible to modify these multilayer AR coating designs for other PV absorber materials.

The performance and durability of these multilayer AR coatings, deposited using pulsed-DC magnetron sputtering, have been investigated. Pulsed-DC magnetron sputtering deposits hard, dense thin films with excellent uniformity. It is possible to control the thickness of each layer with time only using computer control. Abrasion resistance tests have been conducted to evaluate the durability of these coatings. Abrader materials including Felt pad, CS-10 and CS-8, all of which are used in industrial standard tests to simulate the effects of cleaning processes. The tests with a Felt pad were adapted from BS EN 1096 [26]. A Felt pad abrader is the least aggressive material used in this study. Whereas, a CS-10 abrasive material is a rubber pad which applies a mild to medium abrasion and CS-8 abrader provides a medium abrasion [27]. A Spectrophotometer, Optical Microscope, Scanning Electron Microscope (SEM), and Scanning White Light Interferometry (SWLI) were used to investigate the optical and mechanical performance of the coatings.

2. EXPERIMENTAL

Multilayer AR coatings were deposited at Loughborough University using pulsed-DC magnetron sputtering. A “PV Solar” system (from PowerVision, Ltd.) was used to deposit AR coatings on 5x5 cm soda lime glass substrates [28]. The substrates were placed on a rotating carrier and then loaded into the deposition chamber via a load lock. Multilayer broadband AR coatings investigated in this study are listed in Table 1.

Table 1. Multilayer AR Coatings and their applications.

Coating	Description	Application
A	AR 4-layer SiO ₂ /ZrO ₂	Thin film CdTe solar cells
B	AR/IR 4-layer SiO ₂ /ITO	Si solar cells
C	AR 6-layer SiO ₂ /ZrO ₂	Si solar cells

SiO₂ has been used as a low index material and ZrO₂ which has high scratch resistance was deposited as a high refractive index material for Coating A as 4-layer for thin film CdTe solar cell applications. SiO₂ low index material and ITO as a high refractive index material were deposited for Coating B which has 4-layer and optimised for Si solar cells. Coating C has 6-layer of SiO₂ and ZrO₂ for Si solar cells.

A Taber abrader (5900 Reciprocating abrader) shown in Figure 1 was used to test the linear abrasion resistance of the multilayer AR coatings.



Figure 1. A Taber Abrader

Felt pad, CS-10 and CS-8 shown in Figure 2 were used as abrader materials for simulating the cleaning process.



Figure 2. (a) Felt pad, (b) CS-10, (c) CS-8.

The stroke length was 30 mm, and speed was set as 60 cycles per minute. A range of loads from 1 N to 10 N was applied for 50 cycles as shown in Table 2. Lower maximum loads were used for CS-10 and CS-8 abrasers as they are more aggressive materials.

Table 2. List of experiments.

Coating	Abrader	Loads applied
A, B, C	Felt pad	1 N, 2 N, 5 N, 10 N
A, B, C	CS-10	1 N, 2 N
A, B, C	CS-8	1 N, 2 N

Following the abrasion resistance tests, the coatings were cleaned with de-ionized (DI) water and a brush to remove excess material. A Varian Cary 5000 UV-Vis-NIR spectrophotometer was used to measure the reflectance of the coatings before and after the abrasion resistance tests. The wavelength range was between 200 to 1200 nm. Eq. [1] was used to calculate the WAR from the measured data [29], where λ_{min} is the minimum wavelength, λ_{max} is the maximum wavelength, ϕ is the photon flux, R is the reflectance and $d\lambda$ is the differential wavelength.

$$WAR (\lambda_{min}, \lambda_{max}) = \int_{\lambda_{min}}^{\lambda_{max}} \frac{\phi \cdot R}{R} d\lambda \quad [1]$$

An Olympus CX41 optical microscope was used to observe the surface degradation of the coatings. The magnification of the lenses was $\times 10$. An Infinity 2 camera and Infinity Analyse software were used to obtain the images. A Jeol 7100 F and Leo 1530 VP Field Emission Gun (FEG)- SEM were used to analyse the surface damage caused to the coatings. The samples were pasted with silver on metal stubs and then a sputter coater was used to coat a palladium-gold alloy layer on the coatings prior to SEM measurements. A Bruker NPFlex SWLI was used to characterize the surface roughness of the coatings before and after the scratch resistance tests. Three-dimensional (3D) images were generated, and the roughness profile parameters including the root-mean-square (rms) deviation (R_q), and total height (P_t) were calculated.

3. RESULTS AND DISCUSSION

In this study, three types of coatings have been investigated. A Felt pad abrader material was applied to the coatings with a force of 1 N for 50 strokes with a speed of 60 cycles per minute and a stroke length of 30 mm. There was no visible damage observed. The WAR measurements showed no serious degradation as shown in Table 3.

Table 3. WAR measurements of Coating A, B and C after abrasion resistance tests.

Abrader	Load	Coating A	Coating B	Coating C
Increase on WAR (%)				
Felt pad	1 N	0.07	0	0
CS10	1 N	1.5	0.12	0.14
CS10	2 N	2.26	0.44	0.23
CS8	1 N	3.2	0.7	0.61

A CS-10 abrasive material simulates a mild to medium abrasion. This material was used for the scratch resistance testing under 1 N and 2 N loads. The increase in WAR is due to minor damage to the multilayer AR coating after the testing. The CS-8 medium abrader showed a more serious increase in the WAR measurements. Figure 3 compares the WAR data of three coatings after abrasion with CS-10 under 1 N and 2 N loads.

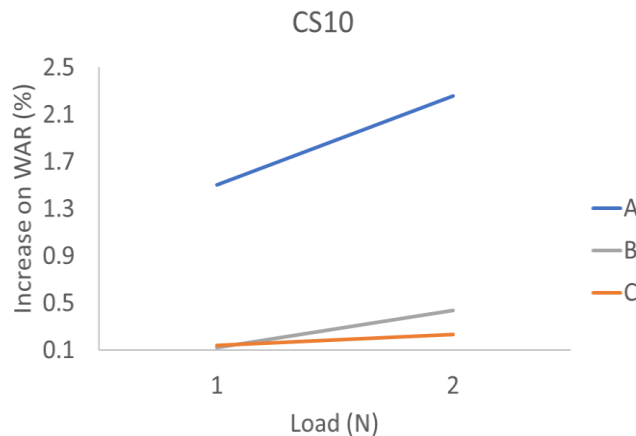


Figure 3. Change on WAR as a function of 1 N and 2 N loads applied with CS-10.

WAR showed an increase for all the coatings when a higher force was applied. Figure 4 presents the optical microscope images of the surface of Coating C; abraded with a Felt pad, CS-10 and CS-8 respectively under 1 N load.

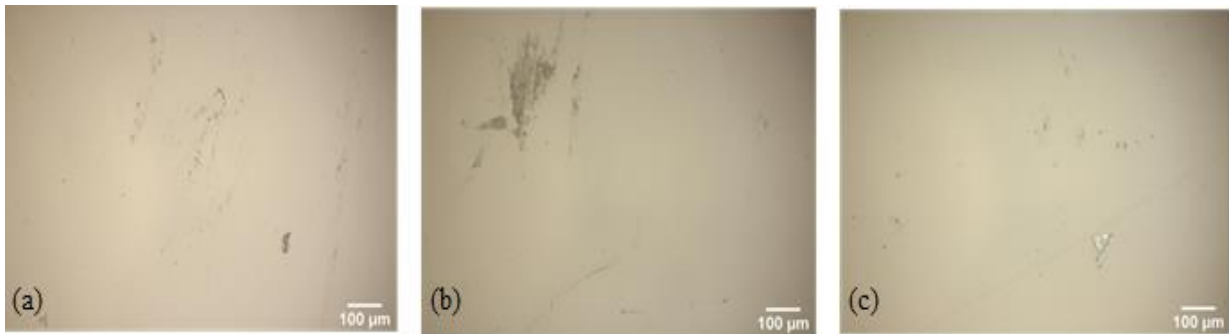


Figure 4. Optical Microscope images of Coating C abraded with (a) Felt pad, (b) CS-10, (c) CS-8. 1 N force was applied.

The images show that coatings were not severely damaged after the abrasion resistance tests. Coating B abraded with Felt pad, CS-10 and CS-8 under 1 N load and the optical microscope images are shown in Figure 5.

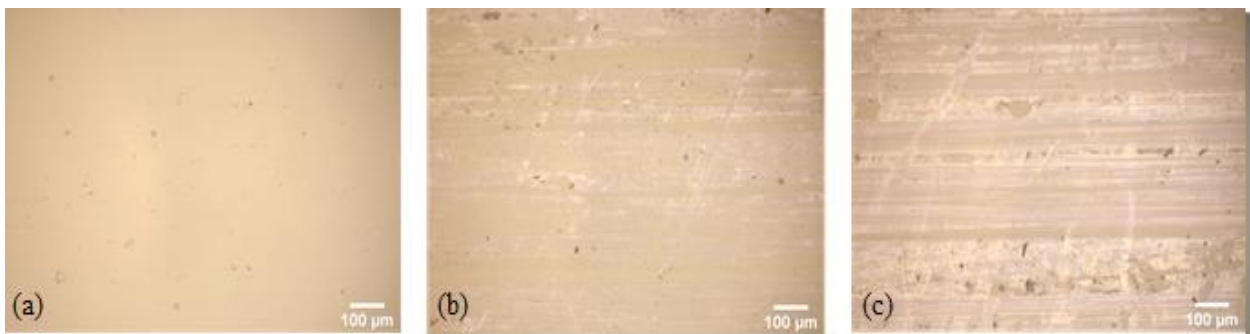


Figure 5. Optical Microscope images of Coating B abraded with (a) Felt pad, (b) CS-10, (c) CS-8. 1 N force was applied.

It was anticipated that more damage would be observed on Coating B compared to Coating A or C due to the inclusion of ITO layers. This may be due to the inclusion of ITO which has inferior hardness to ZrO_2 . In other words, ITO is not as scratch resistant as ZrO_2 . The optical microscope was also used to identify any significant difference observed before and after cleaning the coatings. Figure 6(a) was obtained after Coating B was abraded with a Felt pad under 10 N load. Then the coating was cleaned with DI water and a brush. As shown in Figure 6(b), residues from the abraded material were cleaned and no defect was then visible.

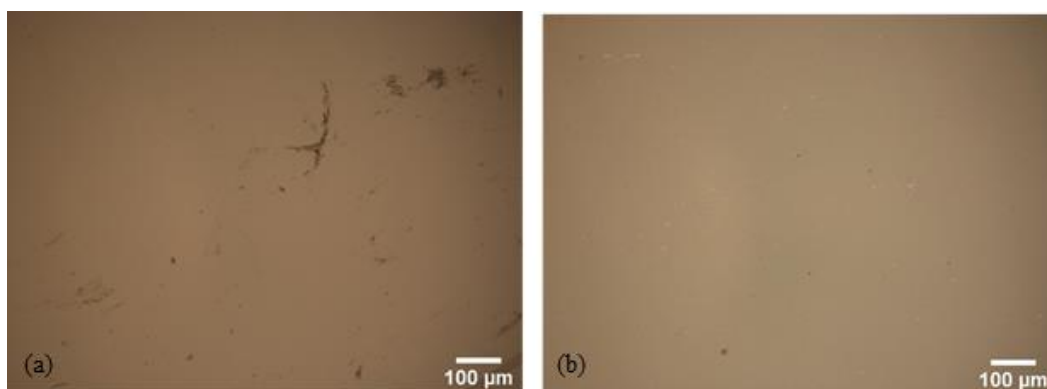


Figure 6. Optical microscope images of coating B (a) after abrasion with a Felt pad under 10 N load, (b) after cleaned with DI water.

Cleaning improved the performance of the coating by removing the dust or any particles left from the abrasion. However, scratches due to the abrasion resistance tests remain as permanent defects. Figure 7 indicates the increase in WAR measurements after abrasion with CS-10.

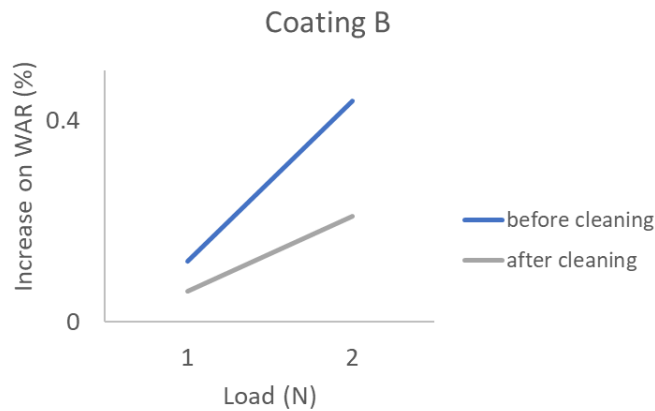


Figure 7. WAR measurements of Coating B after abrasion with CS-10 under 1 N load.

The forces of 1 N and 2 N were applied on coating B. WAR was measured immediately following the abrasion test and then cleaned with DI water and a brush. The data shows that when higher loads are applied, the WAR increases. Moreover, cleaning the samples also lowered the WAR due to removal of residue.

Coating B was abraded with a Felt pad under 1 N, 10 N load, and CS-8 under 1 N load. The SEM images of the abraded surfaces are shown in Figure 8. Felt pad is a soft material and the most suitable abrader for PV cleaning process. However, a range of abrasive materials is required for comparison and testing the performance and durability of these coatings. C-10 and C-8 are more aggressive abrasive materials used in industry. These types cause severe damages to the coatings. When 1N and 2N loads were applied, there were already severe damages on the coatings. The coatings would degrade more and maybe peeled off under higher loads such as 5N or 10N. Therefore, we did not run the tests with loads higher than 2N.

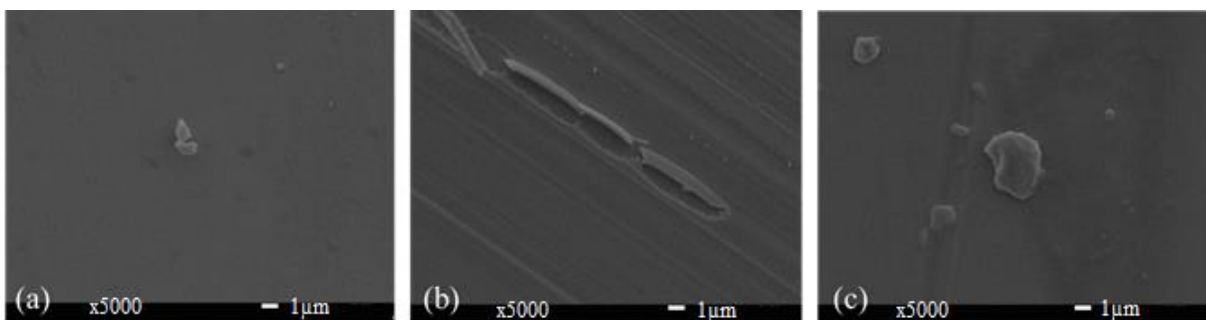


Figure 8. SEM images showing the defects on Coating B after abrasion with (a) Felt pad 1 N load, (b) Felt pad under 10N load, (c) CS-8 under 1 N load.

When the Felt pad abrader was applied with a force of 1 N, there were no defects observed on Coating B. However, when a 10 N load was applied, the coating was damaged, and peeling was observed. The CS-8 abrader under 1 N load also caused scratches on the coating.

A Felt pad and the CS-8 abrader materials were used with the linear abrasion tester to simulate the cleaning effect on Coating C. The Felt pad abrader was applied under 1 N and 10 N loads and CS-8 was tested with a force of 1 N. The SEM images are shown in Figure 9(a,b,c), respectively.

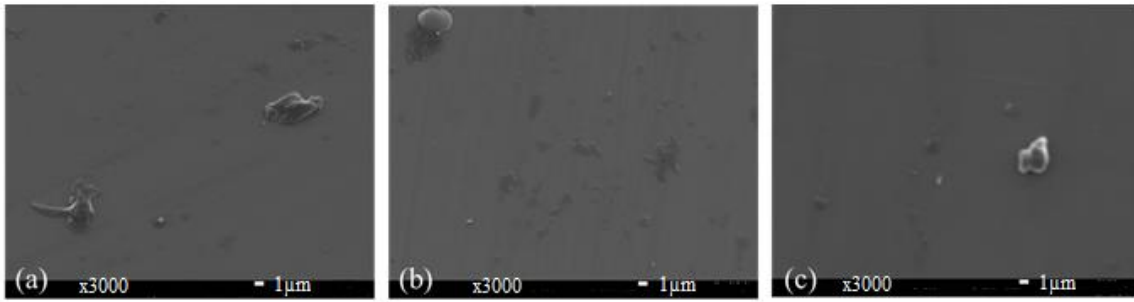


Figure 9. SEM images showing the defects on Coating C after abrasion with (a) Felt pad under 1 N load, (b) Felt pad under 10N load, (c) CS-8 under 1 N load.

The images do not show any scratches or damage to the coatings. It was observed that while Coating B showed severe defects on the coatings, Coating C was more stable after abrasion tests due to its higher scratch resistance. Figure 10 demonstrates SEM images of all three coatings after abraded with CS-10 under 1 N load.

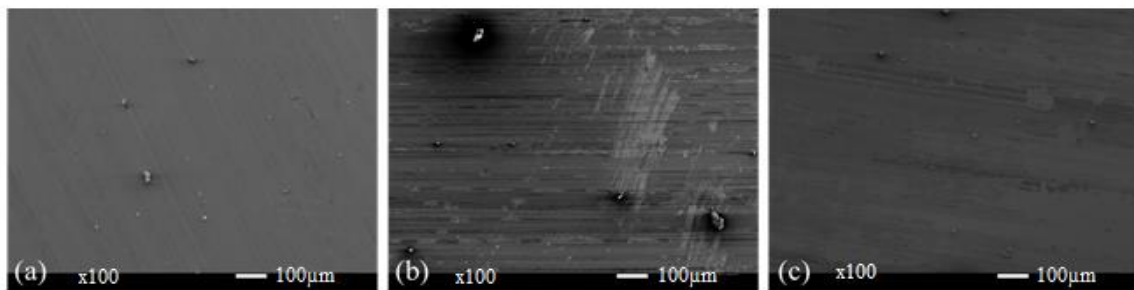


Figure 10. SEM images showing the defects on (a) Coating A, (b) Coating B, (c) Coating C after abrasion with CS-10. 1 N force was applied.

It was observed that there were several scratches on Coating B. Coating A and C had minor defects and fewer scratches however these coatings are more consistent than Coating B. The reason of having less damage on Coating A and C is that these coatings have better scratch resistance as they contain ZrO_2 , a harder material than ITO.

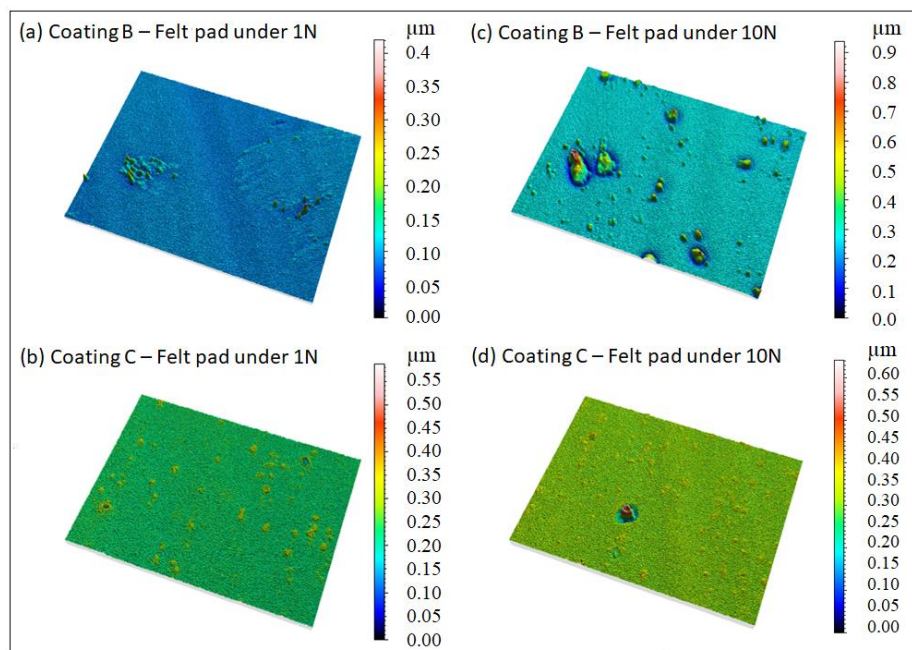


Figure 11. SWLI images showing the scratches after abrasion with Felt pad (a) Coating B under 1 N load, (b) Coating C under 1 N load, (c) Coating B under 10 N load, and (d) Coating C under 10 N load.

SWLI was used to analyse the surface roughness of Coating A, B and C after abrasion with the linear abrasion tester. 3D images were generated to observe the scratches on the coatings. Figure 11 indicates the roughness of Coating B and C after abrasion with the Felt pad under applied forces of 1 N and 10 N.

The coatings remained quite smooth under 1 N load however the roughness increased when a higher force was used. The maximum depth of the scratches occurring on Coating B and C after abrasion under different loads is shown in Figure 12.

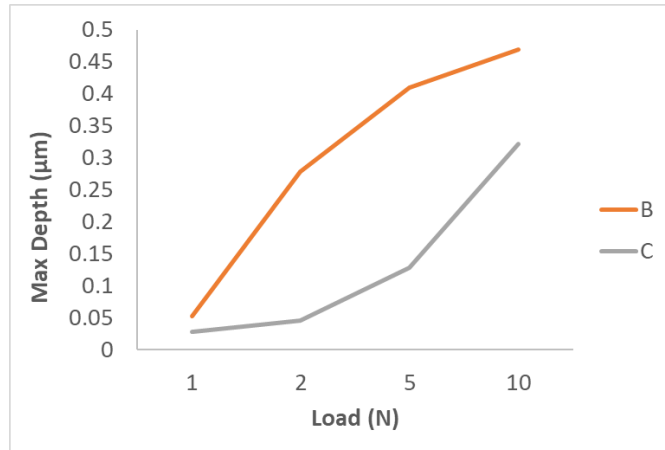


Figure 12. Maximum depth profile of abraded scratches as a function of loads applied.

It was observed that when higher loads were applied, the depth of the scratches also increased. SWLI images are shown in Figure 13 to compare the roughness of Coating B and Coating C after abrasion with CS-8 under 1 N load.

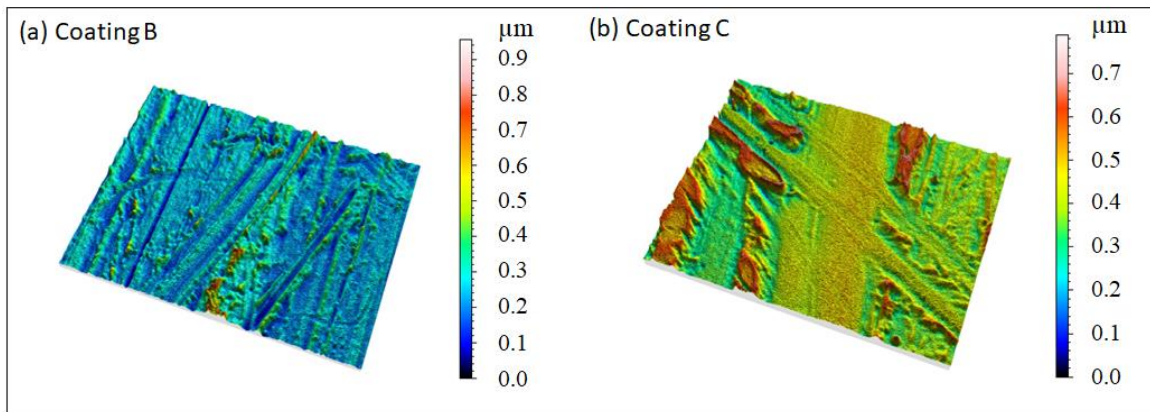


Figure 13. SWLI images showing the scratches on (a) Coating B and (b) Coating C after abraded with CS-8 under 1 N load.

CS-8 is an aggressive material therefore is not surprising that there were several scratches observed on both coatings. The maximum depth and total height of the scratches of Coating B and C abraded with CS-8 under 1 N and 2 N loads are shown in Figure 14.

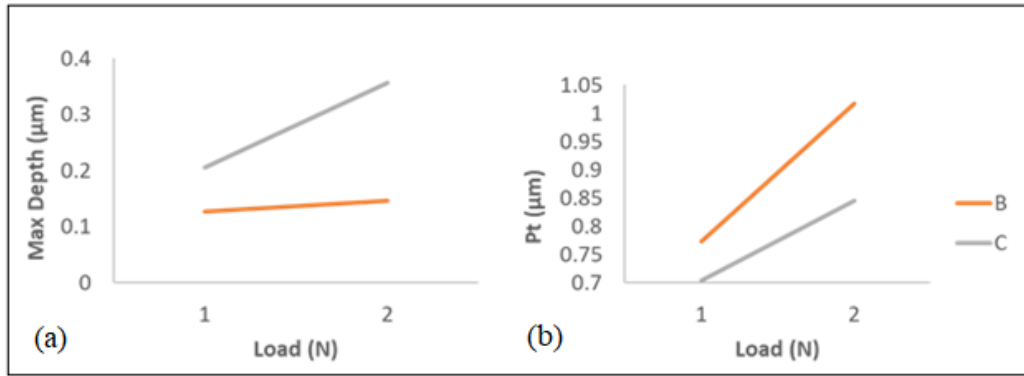


Figure 14. (a) Maximum depth, and (b) Pt profile as a function of loads applied for Coating B and C.

It was observed that when higher loads are applied, the depth of the scratches increased. The maximum depth was higher for Coating C and A compared to Coating B. Furthermore, Pt, the vertical length between the maximum peak height and maximum valley depth, showed an increase when higher loads were applied during abrasion testing. Pt of Coating B was higher than Coating C. Not only scratches but also peeling and residues such as remaining abraded material or dust may affect the Pt. This might explain the higher Pt for Coating B compared to Coating C.

SWLI images of all three coatings are compared in Figure 15 and it was surprisingly observed that there were deeper scratches on Coating A and C whereas the scratches were not as deep on Coating B although more scratches were observed.

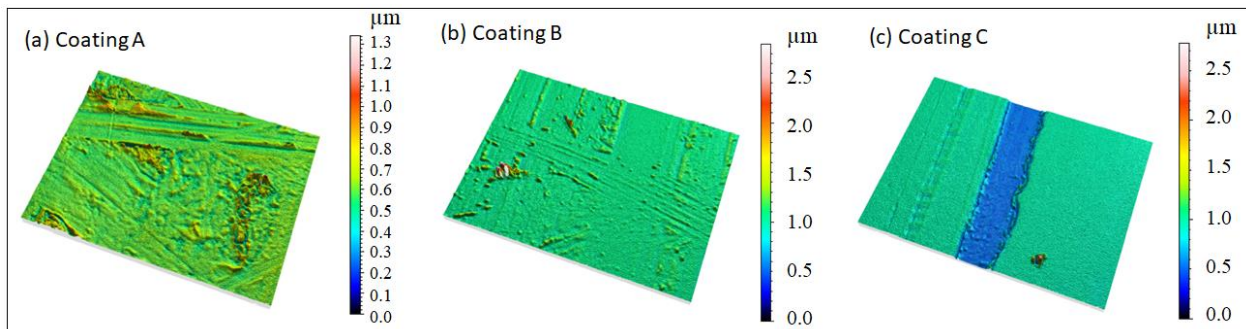


Figure 15. SWLI images showing the scratches of (a) Coating A, (b) Coating B, and (c) Coating C after abrasion with CS-10 under 1 N load.

The roughness profile parameters were calculated. The width, maximum depth and mean depth parameters of all three coatings abraded with CS-10 under 1 N load are given in Table 4.

Table 4. Profile parameters of the scratches observed with SWLI.

Parameters	Coating A	Coating B	Coating C
Width (μm)	5.364	0.612	5.324
Maximum depth (μm)	0.323	0.075	0.445
Mean depth (μm)	0.265	0.071	0.423

The width of the scratches on Coating A and C were over 5 μm, whereas it was only 0.612 μm for Coating B. It was found that roughness increases when more aggressive abraded materials are used or higher forces are applied.

A magnesium fluoride (MgF₂) AR coating was designed by NREL however it is not effective over a broader wavelength [30]. Moreover, an MgF₂ coating is not durable for use in the outdoor environment. ZrO₂ and SiO₂ coatings are more durable and already used in ophthalmic industry [31]. Spin-coated ZrO₂ and spray-deposited TiO₂ MAR coatings were deposited for crystalline silicon solar cells [32].

However, pulsed-DC magnetron sputtering has not been used to deposit uniform and dense MAR coatings before. This study shows similar observations with the findings on durability of Coating A, a 4-layer $\text{SiO}_2/\text{ZrO}_2$ [33]. Moreover, it was extended to analyse and compare the results with Coating B composed of 4-layer SiO_2/ITO and with Coating C, a 6-layer $\text{SiO}_2/\text{ZrO}_2$. The WAR of coatings abraded with a Felt pad under 1 N load were largely undamaged. However, increasing the applied force during tests does increase the WAR for all coatings. Using CS-10 and CS-8 abraders increases the WAR due to minor defects or scratches caused to the multilayer AR coatings. Optical microscope images show that minor scratches occurred on coating C, whereas there was more severe damage observed on Coating B. Coating A and C did not show significant damage after testing with the abrader. The surface roughness of Coating B and C were smooth after abrasion with a Felt pad under 1N load, however, the roughness and the depth of scratches increased when a CS-8 abrader was used. It was unexpected that the maximum depth of the scratches on Coating A and C was higher compared to Coating B. However, a larger number of scratches were observed on Coating B. The outcomes obtained from this study demonstrate that Coating A and C resulted in higher scratch resistance compared to Coating B. However, multilayer AR coatings are more resilient and scratch resistant than single layer sol-gel AR coatings.

4. CONCLUSIONS

Improving the performance and durability of multilayer AR coatings is important for the PV industry. These coatings can reduce the reflection losses and improve module efficiency. It is important that these coatings withstand environmental stresses and are durable to withstand the cleaning processes applied during maintenance. In this study, three different coatings were examined using a linear abrasion tester with a variety of abraders under different loads to investigate the effect of cleaning processes on multilayer AR coatings. These coatings deposited with pulsed DC are 4-layer $\text{SiO}_2/\text{ZrO}_2$ (coating A), 4-layer SiO_2/ITO (Coating B), and 6-layer $\text{SiO}_2/\text{ZrO}_2$ (Coating C). Coating A and C were more durable compared to Coating B. The results demonstrate that using more aggressive abraders or higher loads caused more surface damage and increased surface roughness. The WAR increased for all coatings after the linear abrasion resistance test. The outcomes obtained from this study demonstrate that Coating A and C resulted in higher scratch resistance compared to Coating B, as they contain ZrO_2 which is more scratch resistant than ITO. However, all of the multilayer AR coatings studied here are more resilient and scratch resistant than single layer sol-gel AR coatings which have been shown to be vulnerable to abrasion damage. Their adoption by glass or module manufacturers would improve the performance and lifetime of PV panels. These coatings will now be tested in outdoor conditions in Turkey to correlate outdoor environmental tests with accelerated laboratory tests.

REFERENCES

- [1] Gupta, P, Pandey, A, Vairagi, K, Mondal, SK. Solving Fresnel equation for refractive index using reflected optical power obtained from Bessel beam interferometry. *Review of Scientific Instruments* 2019; 90(1): 015110. DOI: 10.1063/1.5043240
- [2] Van den Berg, PM, Fokkema, JT. The Rayleigh hypothesis in the theory of diffraction by a perturbation in a plane surface. *Radio Science* 1980; 15(4): 723–732. DOI: 10.1029/RS015i004p00723
- [3] Lien, S, Wu, D, Yeh, W, Liu, J. Tri-layer antireflection coatings ($\text{SiO}_2/\text{SiO}_2\text{-TiO}_2/\text{TiO}_2$) for silicon solar cells using a sol-gel technique. *Solar Energy Materials & Solar Cells* 2006; 90(16): 2710–2719. DOI: 10.1016/j.solmat.2006.04.001
- [4] Vincent, A, Babu, S, Brinley, E, Karakoti, A, Deshpande, S, Seal, S. Role of Catalyst on Refractive Index Tunability of Porous Silica Antireflective Coatings by Sol-Gel Technique. *Journal of Physical Chemistry C* 2007; 111(23): 8291–8298. DOI: 10.1021/jp0700736
- [5] Chhajed, S, Schubert, MF, Kim, JK, Schubert, EF. Nanostructured multilayer graded-index antireflection coating for Si solar cells with broadband and omnidirectional characteristics. *Applied Physics Letters* 2008; 93(25): 251108. DOI: 10.1063/1.3050463
- [6] Prieto-Castrillo, F, Núñez, N, Vázquez, M. Warranty assessment of photovoltaic modules based on a

- degradation probabilistic model. *Progress in Photovoltaics: Research and Applications* 2020; 28(12): 1308–1321. DOI: 10.1002/pip.3328
- [7] Sevinc, PC, Albayrak, FS, Bagriyanik, M, Batman, A. Lifetime and Efficiency Concerns of a Photovoltaic Power. In: ECRES 2015 3. European Conference on Renewable Energy Systems; 7-10 October 2015: Vizyon Publishing House, pp. 1–6.
- [8] Womack, G, Kaminski, PM, Abbas, A, Isbilir, K, Gottschalg, R, Walls, JM. Performance and durability of broadband antireflection coatings for thin film CdTe solar cells. *Journal of Vacuum Science & Technology A: Vacuum, Surfaces, and Films* 2017; 35(2): 021201. DOI: 10.1116/1.4973909
- [9] Ilse, K, Pfau, C, Miclea, PT, Krause, S, Hagendorf, C. Quantification of abrasion-induced ARC transmission losses from reflection spectroscopy. In: 2019 46th IEEE Photovoltaic Specialists Conference; 16-21 June 2019:IEEE, pp. 2883–2888.
- [10]Phillips, BM, Jiang, P. Biomimetic Antireflection Surfaces. In: Lakhtakia A, Martin-Palma R, editors. *Engineered Biomimicry*, Florida, USA: Elsevier, 2013, pp. 305-331.
- [11]Rubin, M. Optical properties of soda lime silica glasses. *Solar Energy Materials and Solar Cells* 1985; 12(4): 275–288. DOI: 10.1016/0165-1633(85)90052-8
- [12]Womack, G, Kaminski, PM, Walls, JM. Optical optimization of high resistance transparent layers in thin film cadmium telluride solar cells. *Vacuum* 2017; 139: 196–201. DOI: 10.1016/j.vacuum.2016.11.031
- [13]Kosyachenko, LA, Grushko, EV, Mathew, X. Quantitative assessment of optical losses in thin-film CdS/CdTe solar cells. *Solar Energy Materials and Solar Cells* 2012; 96: 231–237. DOI: 10.1016/j.solmat.2011.09.063
- [14]Law, AM, Wright, LD, Smith, A, Isherwood, PJM, Walls, JM. 2.3% Efficiency Gains for Silicon Solar Modules Using a Durable Broadband Anti-reflection Coating. In: 2020 47th IEEE Photovoltaic Specialists Conference; 15-21 August 2020:IEEE, pp. 0973–0975.
- [15]Mehmood, U, Al-Sulaiman, FA, Yilbas, BS, Salhi, B, Ahmed, SHA, Hossain, MK. Superhydrophobic surfaces with antireflection properties for solar applications: A critical review. *Solar Energy Materials and Solar Cells* 2016; 157: 604–623. DOI: 10.1016/j.solmat.2016.07.038
- [16]Shanmugam, N, Pugazhendhi, R, Madurai Elavarasan, R, Kasiviswanathan, P, Das, N. Anti-Reflective Coating Materials: A Holistic Review from PV Perspective. *Energies* 2020; 13(10): 2631. DOI: 10.3390/en13102631
- [17]San Vicente, G, Bayón, R, Germán, N, Morales, A. Long-term durability of sol–gel porous coatings for solar glass covers. *Thin Solid Films* 2009; 517(10): 3157–3160. DOI: 10.1016/j.tsf.2008.11.079
- [18]Bouhafs, D. Design and simulation of antireflection coating systems for optoelectronic devices: Application to silicon solar cells. *Solar Energy Materials and Solar Cells* 1998; 52(1–2): 79–93. DOI: 10.1016/S0927-0248(97)00273-0
- [19]Chen, D. Anti-reflection (AR) coatings made by sol–gel processes: A review. *Solar Energy Materials and Solar Cells* 2001; 68(3–4): 313–336. DOI: 10.1016/S0927-0248(00)00365-2
- [20]Khan, SB, Irfan, S, Zhuanghao, Z, Lee, SL. Influence of refractive index on antireflectance efficiency of thin films. *Materials* 2019; 12(9): 8–10. DOI: 10.3390/ma12091483
- [21]Ali, K, A. Khan, S, Jafri, MZM. Effect of Double Layer (SiO₂/TiO₂) Anti-reflective Coating on Silicon Solar Cells. *International Journal of Electrochemical Science* 2014; 9:7865–7874.
- [22]Ul-Hamid, A. The effect of deposition conditions on the properties of Zr-carbide, Zr-nitride and Zr-carbonitride coatings – a review. *Materials Advances* 2020; 1(5): 988–1011. DOI: 10.1039/D0MA00232A
- [23]Walls, M. Optical coatings for ophthalmic lenses by reactive magnetron sputtering. In: *Optical Interference Coatings*; 15 July 2001:Optical Society of America, pp. ThD1.
- [24]Law, AM, Kaminski, PM, Isherwood, PJM, Walls, JM. An Infra-red Reflecting Optical Coating for Solar Cover Glass. In: 2019 IEEE 46th Photovoltaic Specialists Conference; 16-21 June 2019:IEEE, pp. 1913–1918.
- [25]Javed, A. The Effect of Temperatures on the Silicon Solar Cell. *International Journal of Emerging Technologies in Computational and Applied Sciences* 2014; 3(9): 305–308.
- [26]British Standards Institute. BS EN 1096-2:2012. Glass in building - Coated glass Part 2: Requirements and test methods for class A, B and S coatings. London: British Standards Institute, 2012.
- [27]American Society for Testing and Materials. ASTM TM D4060-14. Standard Test Method for Abrasion Resistance of Organic Coatings by the Taber Abraser. ASTM International, West Conshohocken, PA, 2014.
- [28]Lisco, F, Kaminski, PM, Abbas, A, Bowers, JW, Claudio, G, Losurdo, M, Walls, JM. High rate deposition of thin film cadmium sulphide by pulsed direct current magnetron sputtering. *Thin Solid Films* 2015; 574:43–51. DOI: 10.1016/j.tsf.2014.11.065
- [29]Lind, MA, Pettit, RB, Masterson, KD. The Sensitivity of Solar Transmittance, Reflectance and Absorptance to Selected Averaging Procedures and Solar Irradiance Distributions. *Journal of Solar Energy Engineering* 1980; 102(1): 34–40, DOI: 10.1115/1.3266119
- [30]Wu, X, Keane, JC, Dhere, RG, Dehart, C, Albin, DS, Duda, A, Gessert, TA, Asher, S, Levi, DH, Sheldon, P. High-Efficiency CTO/ZTO/CdS/CdTe Polycrystalline Thin-Film Solar Cells. Proc. 17th Photovoltaic Sol. Energy Conf. Exhib. 2001; pp. 995-1000.

- [31] Walls, JM, Spencer, AG. Hard coating and the durability of anti-. reflection coatings. *Opt. World*. 2000; 29:40.
- [32] Uzum, A, Kuriyama, M, Kanda, H, Kimura, Y, Tanimoto, K, Fukui, H, Izumi, T, Harada, T, Ito, S. Sprayed and Spin-Coated Multilayer Antireflection Coating Films for Nonvacuum Processed Crystalline Silicon Solar Cells. *International Journal of Photoenergy* 2017; 1–5. DOI: 10.1155/2017/3436271.
- [33] Newkirk, JM, Nayshevsky, I, Sinha, A, Law, AM, Xu, Q, To, B, Ndione, PF, Schelhas, LT, Walls, JM, Lyons, AM, Miller, DC. Artificial linear brush abrasion of coatings for photovoltaic module first-surfaces. *Solar Energy Materials and Solar Cells* 2021; 219:110757. DOI: 10.1016/j.solmat.2020.110757